Towards a Generalized Neural Network Approach for Identifying Critical Wave Groups

Kevin M. Silva, *David Taylor Model Basin (NSWCCD); University of Michigan*

kevin.m.silva14.civ@us.navy.mil

Kevin J. Maki, *University of Michigan* kjmaki@umich.edu

ABSTRACT

Ships will experience an assortment of harsh ocean environments throughout their lifetime and will be tasked with navigating these circumstances under different operating conditions (e.g. speed, heading, maneuver). Traditional extreme event probabilistic models typically focus on a single description of the seaway and operating condition to perform analyses. However, large amounts of experimental or computational resources are needed to cover the span of all the conditions a vessel could encounter. The objective of current work is to extend the CWG-CFD-LSTM framework from Silva et al. (2022) to multiple speeds and headings for a free-running vessel. The CWG-CFD-LSTM framework combines the critical wave groups method (CWG), computational fluid dynamics (CFD), and long short-term memory (LSTM) neural networks to develop computationally efficient surrogate models than can predict the six degree of freedom (6-DoF) temporal response of the vessel and recover the extreme statistics. Two modelling approaches are considered. A general model approach where one model is trained with all the speeds and headings and an ensemble model approach where multiple models are trained, each responsible for a single speed and heading combination. The extended framework is demonstrated on a case study with simulations from the Large Amplitude Motion Program (LAMP) of the David Taylor Model Basin (DTMB) 5415 hull form operating in Sea State 7 at different speeds and headings. The developed neural network models with the general approach are capable of accurately representing the temporal response of the free-running DTMB 5415 in extreme waves and also recovering the extreme statistics of roll for different speeds and headings.

Keywords: *Extreme Events, Neural Networks, Ship Hydrodynamics, Machine Learning*

1. INTRODUCTION

The probabilistic quantification of extreme ship response events is a critical consideration in the design of new vessels and in the development of operational guidance of existing vessels. Vessels will not only experience a variety of wave environments in their lifetime but will also undergo a variety of operations as well which will require different speeds, headings, and maneuvers. Traditionally, extreme event probabilistic methodologies have only focused on quantifying the occurrence of extreme events for a singular operating and wave condition. Though focusing on a single operating and wave condition greatly simplifies the probabilistic evaluations and is often necessary, the quantity of data required to evaluate the extremes for multiple conditions scales linearly with the quantity of conditions and the analysis for one condition is completely independent of others.

Conventional extreme event predicting frameworks all suffer from this lack of generalization in terms of operating and wave conditions. These methods include extrapolation-type methods (Campbell and Belenky, 2010a,b; Belenky and Campbell, 2011), perturbation methods like the split-time method (Belenky, 1993; Belenky et al. 2010; Weems et al. 2020), and wave group methods

like the critical wave groups (CWG) method (Themelis and Spyrou, 2007; Anastopoulos et al., 2016; Anastopoulos and Spyrou, 2016, 2017, 2019), sequential sampling methods from Mohamad and Sapsis (2018), and the Design Loads Generator (DLG) (Alford, 2008).

Additionally, evaluations must be performed for nominal operating and environmental conditions, that may not be representative of real-time wave environments on-board a vessel. The computational cost of accurate ship hydrodynamics simulation tools also prevents any real-time extreme event probabilistic evaluations given the instantaneous wave environment and ship's current operating profile and any evaluations will have to rely on analyses for nominal conditions.

For both accurate evaluation of extremes for large quantities of conditions and possibility of real-time extreme event probabilistic quantification, hydrodynamic predictions that are much faster than real-time are required. Accurate hydrodynamic simulation tools are all too computational expensive to produce predictions that are faster than real-time. Therefore, system identification (SI) is necessary to produce fast-running surrogate models. The present work extends previous research by Silva and Maki (2021a,b,c) and Silva et al. (2022) combining the CWG method, computational fluid dynamics (CFD), and long short-term memory (LSTM) neural networks to build a CWG-CFD-LSTM extreme event framework and an LSTM methodology for developing generalized surrogate models for free-running vessels that are free to move in all six degrees of freedom (6-DoF).

The objective of the present work is to develop a generalized framework capable of quantifying the probability of extremes for multiple conditions without the need for large dataset for each individual condition. Two different modelling approaches are considered. A general modelling approach where a single model is trained for all the conditions will be compared against an ensemble model approach where multiple neural network models are trained, each responsible for a single condition. The paper is organized as follows. A summary of the CWG method is presented, followed by a description of the neural network approach and the improved CWG-CFD-LSTM framework. Finally, the improved framework will be demonstrated on a case study with a free-running full-scale David Taylor Model Basin (DTMB) 5415 hull form operating at multiple speeds and headings in Sea State 7 (NATO, 1983) irregular seas.

2. CRITICAL WAVE GROUPS METHOD

The presented improved framework for predicting extreme ship responses events employs the CWG method at its core to both generate the wave groups and calculate the extreme statistics. The present implementation of the CWG method comes from work of Themelis and Spyrou (2007); Anastopoulos et al. (2016); Anastopoulos and Spyrou (2016, 2017, 2019). The main idea behind the CWG method is that the probability of a response ϕ exceeding a critical value ϕ_{crit} is equal to probability of all the wave groups and ship states at the moment of encountering the wave group that lead to an exceedance. The ship state at the moment of encountering the wave group is referred to herein as the encounter condition, sometimes referred to as the initial condition.

Wave groups in the CWG methodology are constructed with Markov chains and the statistical relationship between the heights and periods of successive waves. Given the height and period of any wave, the Markov chain methodology can predict the most likely preceding or following wave. Each wave only depends on the closest successive wave because of the Markov chain's memoryless property. Therefore, a wave group with j waves can be fully described given the height H_c and period T_c of the largest wave in a group,

The CWG method identifies all the wave group and encounter condition pairs that lead to an exceedance. The *critical* wave groups lead to a near-exceedance and any wave groups with larger waves of the same form are assumed to also lead to an exceedance. Therefore, for each encounter condition ec_k and wave group with shape described by T_c and j, there is an H_c that denotes the critical wave group. This variation of H_c to identify a critical wave group is illustrated in Figure 1.

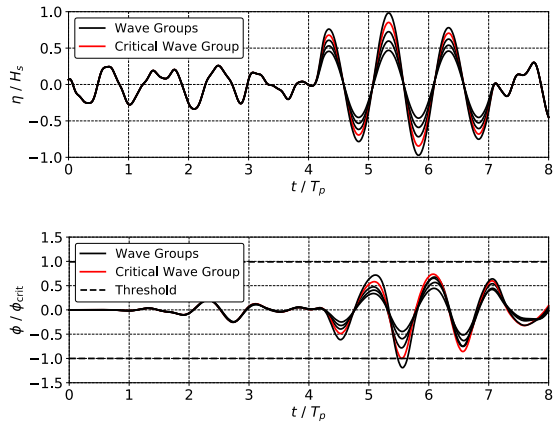

Figure 1. Identification of a critical wave group for a given set of wave groups with similar shapes.

The probability of a response ϕ exceeding a critical value ϕ_{crit} is described Equation 1, where the calculation is a combination of the probability of the k^{th} encounter condition $p[ec_k]$ and the probability that a wave group exceeds the critical wave group $p\left[wg_{m,j}^{(k)}\right]$, for the m^{th} wave period range, j waves in the group and the k^{th} encounter condition.

$$p[\phi > \phi_{\text{crit}}] = \sum_k \sum_m \left(1 - \prod_j \left(1 - p\left[wg_{m,j}^{(k)}\right]\right)\right) \times p[ec_k] \quad (1)$$

More details of the presented implementation of the CWG method wave group construction and probability of exceedance formulation can be found in Anastopoulos and Spyrou (2019) and Silva et al. (2022).

3. NEURAL NETWORK MODEL

The neural network approach in the current work builds of the work of Silva et al. (2022), where LSTM neural networks were demonstrated to represent effectively the 6-DoF response of a vessel within the CWG-CFD-LSTM frame work for a single speed, heading, and seaway description.

The main idea of the current neural network approach that was first developed in Silva and Maki (2022), is that the 6-DoF response of a vessel depends on the waves that are encountered in the instantaneous encounter frame. However, the instantaneous encounter frame is not known *a priori*, thus it must be estimated. Estimations of the encounter frame can be made from the nominal speed and heading of the vessel or through the surge, sway, and yaw from the traning data. Figure 2 from Silva and Maki (2022), shows the surge, sway, and yaw time-histories from a set of irregular wave realizations. The mean of all the realizations provides an estimate of the encounter frame and is able to capture any mean drift that may be present in a given dataset.

The input into the LSTM neural network is the wave elevation time-histories at a series of waves probes that move with the estimated frame. Given a probe k, the wave elevation in the estimated encounter frame can be described by:

$$\eta_k(\boldsymbol{x_k}, t) = \sum_n a_n \cos(\omega_n t - \boldsymbol{k}_n) \cdot (\boldsymbol{x_E}(t) + \boldsymbol{R}_E(t) \cdot \boldsymbol{x_k}) + \phi_n \quad (2)$$

where a_n, ω_n, and ϕ_n correspond to the amplitude, frequency, and phase of the wave Fourier components, $\boldsymbol{k_n}$ is a vector describing the wavenumber and direction of each component, $\boldsymbol{x_E}(t)$ is the coordinate location of the estimated encounter frame with respect to time t, $\boldsymbol{x_k}$ is the coordinate location of probe k in the initial earth-fixed frame, and $\boldsymbol{R}_E(t)$ is a rotation matrix describing the mean yaw trajectory with respect to time.

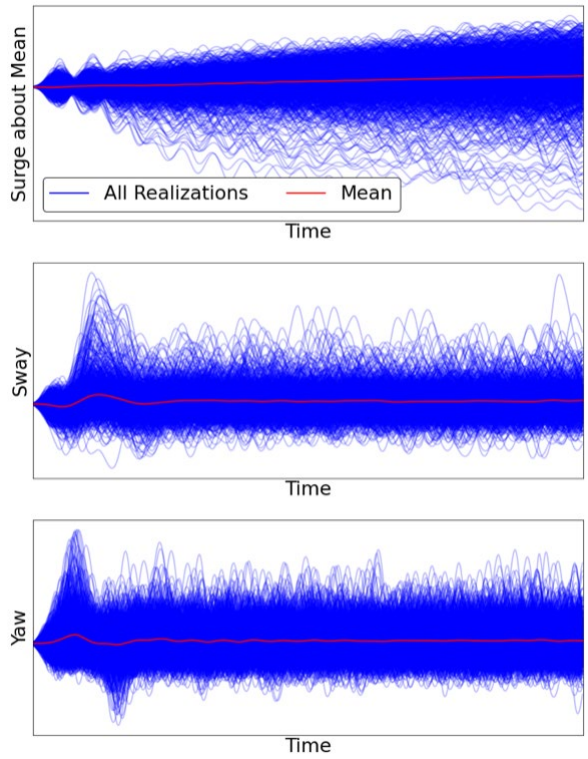

Figure 2. Estimated trajectories for coursekeeping from Silva and Maki (2022).

The full input for the neural network model during training is for K wave probes, M training runs, and T steps and is described in the form of a 3-D matrix as:

$$\boldsymbol{X} = \begin{bmatrix} \boldsymbol{x_{11}} & \boldsymbol{x_{12}} & \cdots & \boldsymbol{x_{1T}} \\ \boldsymbol{x_{21}} & \boldsymbol{x_{22}} & \cdots & \boldsymbol{x_{2T}} \\ \vdots & & \ddots & \vdots \\ \boldsymbol{x_{M1}} & \boldsymbol{x_{M2}} & \cdots & \boldsymbol{x_{MT}} \end{bmatrix} \tag{3}$$

where each component in the input matrix $\boldsymbol{x_{mt}} = \left[x_{mt}^{(1)}, x_{mt}^{(2)}, \ldots, x_{mt}^{(K)}\right]$, corresponds to the wave elevation at time t, for training run m for wave probe 1 through K. The output matrix during training is shaped like the input matrix and is formulated as:

$$\boldsymbol{y} = \begin{bmatrix} \boldsymbol{y_{11}} & \boldsymbol{y_{12}} & \cdots & \boldsymbol{y_{1T}} \\ \boldsymbol{y_{21}} & \boldsymbol{y_{22}} & \cdots & \boldsymbol{y_{2T}} \\ \vdots & & \ddots & \vdots \\ \boldsymbol{y_{M1}} & \boldsymbol{y_{M2}} & \cdots & \boldsymbol{y_{MT}} \end{bmatrix} \tag{4}$$

where each component in the output matrix $\boldsymbol{y_{mt}} = \left[y_{mt}^{(1)}, y_{mt}^{(2)}, \ldots, y_{mt}^{(6)}\right]$, corresponds to the 6-DoF motion values at time t and for training run m. Previous work in Silva and Maki (2022) made the observation that quantities that are slowly varying like surge and sway displacement do not produce as favorable results as DoF such as heave, roll, and pitch. Therefore, the present work defines the 6-DoF vessel response as the surge velocity, sway velocity, heave, roll, pitch, and yaw. With the input and output matrices defined in Equation 3 and 4 respectively, the model is trained to optimize the relationship between $\boldsymbol{X}$ and $\boldsymbol{y}$ with a mean-squared error (MSE) loss function and Adam optimizer (Kingma and Ba, 2014).

The neural network architecture in the following paper follows the work of Silva and Maki (2022) and Silva et al. (2022) with three LSTM layers followed by a dense fully connected layer. Uncertainty estimates were also made in the same manner as Silva and Maki (2022) and Silva et al. (2022) with the Monte Carlo dropout method from Gal and Ghahramani (2016a,b), where dropout layers are employed in between each LSTM layer. Dropout layers are typically used during training to avoid overfitting by randomly and temporarily removing a specified percentage of the neurons in the layer. The Monte Carlo dropout methodology applies the same principle during prediction as well and results in stochastic predictions which enables estimates of the model uncertainty.

The application of the developed neural network methodology for multiple speeds and headings only differs from a single condition method in that each condition has its own estimated frame. Therefore, each training run's wave elevation inputs are considered in the condition-specific encounter frame.

4. CWG-CFD-LSTM FRAMEWORK

The implementation of the CWG method with CFD (CWG-CFD) was first introduced in Silva and Maki (2021a), where a framework was

presented that allowed for the CWG method to be implemented with high-fidelity CFD simulations with unsteady Reynolds-averaged Navier-Stokes (URANS) or even model tests. The CWG-CFD framework solved the issue of enforcing different encounter conditions at the moment of wave group impact by introducing the *natural initial condition* concept. The natural initial condition utilizes previously observed vessel responses from random wave trains to identify encounter conditions of interest and then blends the deterministic wave groups predicted by the Markov chains into the same wave trains in a manner that guarantees that the encounter condition occurs at the start of the wave group. The natural initial condition avoids the need for any intrusive techniques of enforcing the encounter condition by placing all of the focus on the generation of physically realizable composite wave trains that contain embedded Markov chain wave groups.

Though the CWG-CFD method solved the encounter condition problem, it was still computationally expensive because of all the computations involved in identifying critical wave groups. The CWG-CFD-LSTM methodology was introduced in Silva and Maki (2021b,c), where the methodology was identical to the CWG-CFD framework except that surrogate models of the ship dynamical response in the time-domain were built with an LSTM neural network. The surrogate models then are able to simulate a wider range of the composite wave groups and calculate the probabiltiy of exceedance according to Equation 1.

The present work applies the same methodology outlined in Silva and Maki (2021b,c) and the extension to 6-DoF in Silva et al. (2022). However, the current work is focused on building more generalized surrogate models capable of simulating multiple speeds and headings and thus enabling the identification of critical wave groups and extreme events for different conditions.

5. CASE STUDY

The presented methodology for modelling extreme ship motions for different conditions with a general LSTM neural network approach within the CWG-CFD-LSTM framework is demonstrated with simulations performed with the Large Amplitude Motion Program (LAMP) (Lin et al. 1994, 2007) for the DTMB 5415 hull form in Figure 3. The current work utilizes the LAMP-3 formulation, where the hydrodynamics (radiation and diffraction) is solved about the mean wetted surface (body-linear), and the hydrostatics and Froude-Krylov forces are solved over the instantaneous wetted surface (body-nonlinear). The blended nonlinear methodology can resolve a significant portion of nonlinear effects in most ship-wave problems at a fraction of the computational effort for the general body-nonlinear formulation and allows for large lateral motions and simulations of free-running vessels. Though under some definitions, LAMP is not considered to be a CFD tool like a finite volume URANS method, LAMP provides enough fidelity in the solution of the ship-wave interaction problem to provide sufficient nonlinearity and accuracy to test the CWG-CFD-LSTM framework for multiple conditions.

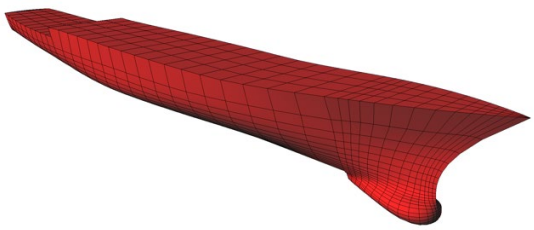

Figure 3. LAMP representation of the DTMB 5415 hullform.

Table 1 lists the loading condition and fluid properties for the DTMB 5415 case study. The loading condition is derived from CFD validation studies performed for the 5415M in Sadat-Hosseini (2015), while the fluid properties represent seawater at 20° (ITTC, 2011). The DTMB 5415 is free to surge, sway, heave, roll, pitch and yaw in the LAMP

simulations. The vessel's forward speed is controlled with a quasi-steady propeller performance model from Lee et al. (2003) and the rudders are modelled as low-aspect ratio foils that are actuated by a proportional-integral-derivative (PID) controller to maintain heading.

Table 1. Loading condition and fluid properties for the DTMB 5415 LAMP simulations.

Properties	Units	Value
Length Between Perp.	m	142.0
Beam	m	19.06
Draft	m	6.15
Displacement	tonnes	8431.8
LCG (+Fwd of AP)	m	70.317
VCG (Above BL)	m	7.51
GMT	m	1.95
Roll Gyradius	m	7.62
Pitch Gyradius	m	35.50
Yaw Gyradius	m	35.50
Density of Water	kg/m^3	1024.81
Kin. Viscosity of Water	m^2/s	1.0508e-6
Accel. due to Gravity	m/s^2	9.80665

Table 2 summarizes the seaway and operating conditions considered in the current work. A database of wave groups is constructed for Sea State 7 long-crested seas described by the JONSWAP spectrum. Four operating conditions of interest are considered in the current work with the different combinations of speeds of 10 and 20 knots and headings of 45 (bow-quartering) and 135 deg (stern-quartering). As done in previous studies with CWG, roll was selected as the quantity of interest with roll and roll velocity selected as the encounter conditions. Random irregular wave simulations were performed for each speed and heading combination to identify wave trains to act as the natural initial condition for selected encounter conditions for the CWG evaluation.

The present paper compares two different neural network modelling approaches to handle the extreme evaluation of different speeds and headings. The general approach utilizes simulations from different speeds and headings, while the ensemble approach builds a separate model for each individual speed and heading combination. The training dataset contains 1920 total simulation runs (192 hours) with 480 training runs (48 hours) per each speed and heading combination. The validation dataset contains a total of 8000 simulations (800 hours), where each speed and heading combination has 2000 validation runs (200 runs). The details of the training and validation matrix, and the neural network architecture and hyper-parameters for both modelling approaches is summarized in Table 3.

Table 2. Operating and seaway conditions for the DTMB 5415 case study

Properties	Units	Value
Speeds	knots	10, 20
Headings	deg	45, 135
Sea State	-	7
Significant Wave Height, H_s	m	9.0
Peak Modal Period, T_p	s	15
Individual Run Length	s	360

Table 3. Training and validation matrix, neural network architecture, and hyper-parameters for the DTMB 5415 case study.

Properties	Value
No. Total Training Runs	60, 120, 240, 480, 960, 1920
No. Training Runs per Condition	15, 30, 60, 120, 240, 480
No. Total Validation Runs	8000
No. Validation Runs per Condition	2000
No. Time Steps per Run	720
No. Wave Probes	27
No. Units per Layer	250
No. Layers	3
Dropout	0.1
Learning Rate	0.00001
No. Epochs	5000
Optimizer	Adam

As detailed in Table 3, models for both modelling approaches are constructed with different quantities of training data to understand the convergence of the models. Each model is evaluated on its respective validation

dataset for the ability to predict the temporal response of the 6-DoF response of the vessel and the ability to produce the same probability of exceedance predictions from a pure CWG-CFD methodology.

All the constructed models were evaluated for their accuracy with respect to training data quantity for both L_2 and L_∞ error, which are described in Equation 5 and 6 respectively for a single run, where T is the number of time steps, y is the LAMP prediction and $\hat{y}$ is the prediction from the neural network. The L_2 error provides an estimate of how the overall response time-history compares between LAMP and the neural network prediction, while the L_∞ error quantifies the maxim difference between LAMP and the neural network prediction for each run.

$$L_2(y,\hat{y}) = \sqrt{\frac{1}{T}\sum_{i=1}^{T}(y_i - \hat{y}_i)^2} \quad (5)$$

$$L_\infty(y,\hat{y}) = \max_{i=1,\ldots,T}|y_i - \hat{y}_i| \quad (6)$$

Figure 4 and Figure 5 are comparisons of L_2 and L_∞ error respectively for both the general and ensemble modelling approaches and for each DoF. For each validation run, the L_2 and L_∞ error was calculated for each DoF. Each marker in Figure 4 and Figure 5 corresponds to the median error for all the validations runs for a particular DoF at the specified training data quantities. The error bars in Figure 4 and Figure 5 correspond to the 25th and 75th percentiles. For both modelling approaches and error quantities, the overall median and spread of error decreases as the training data quantity increases. Overall, the general approach produces lower error than the ensemble approach with less training data. However, the two approaches trend towards each other as the quantity of training data is increased. The only exception is the evaluation of the pitch predictions, where the ensemble approach provides a lower error for all models. Overall, both modelling approaches provide similar L_2 and L_∞ error estimations with larger quantities of training data.

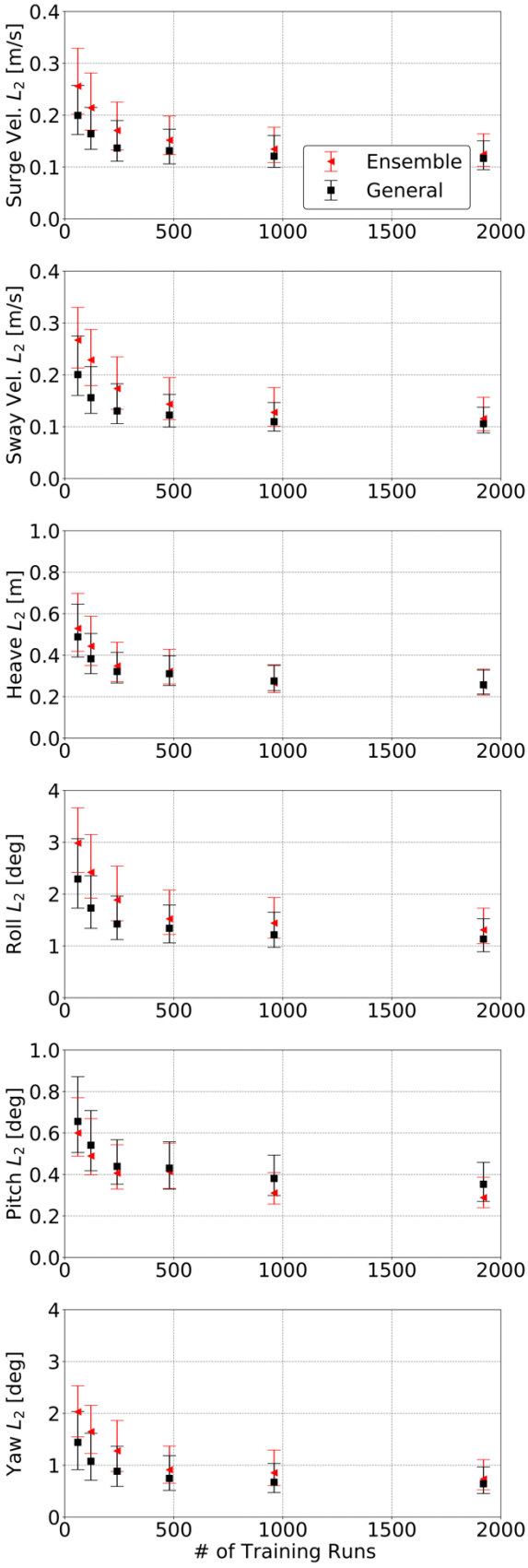

Figure 4. Convergence of neural network models for L_2 error.

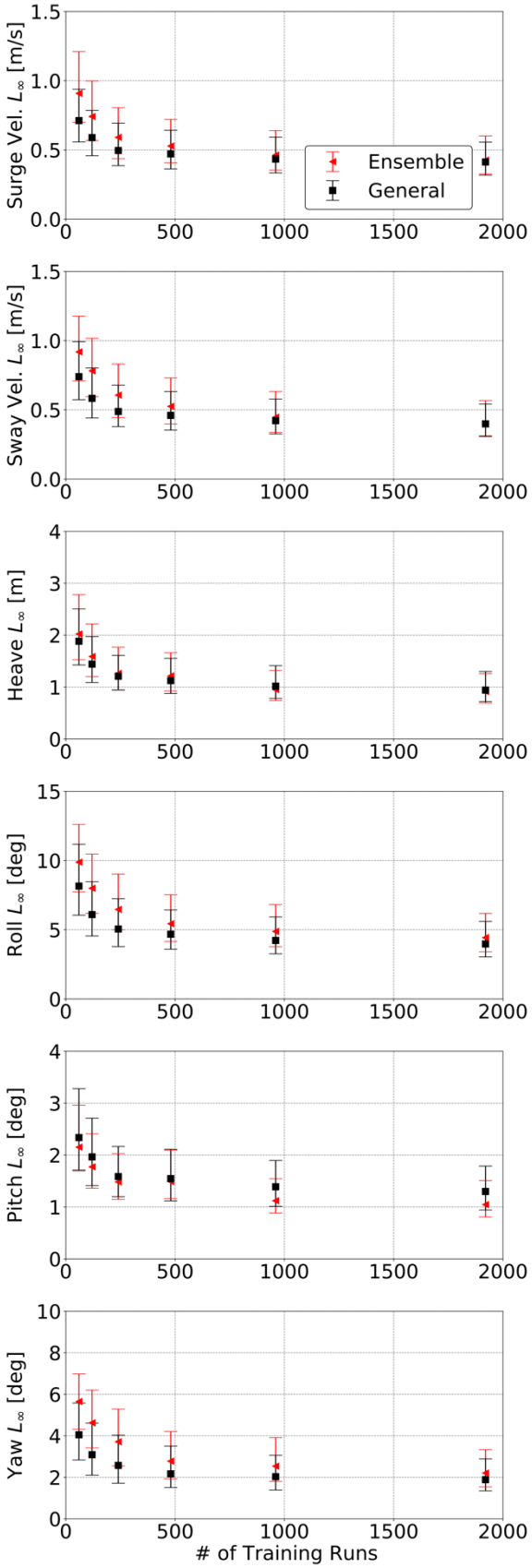

Figure 5. Convergence of neural network models for L_∞ error.

Figure 4 and Figure 5 provided an overall assessment of the accuracy of the developed models with regards to the L_2 and L_∞ error of each validation run. Figure 6 and Figure 7 show time-history comparisons of the validation runs for each DoF with the smallest and largest L_∞ error respectively for a general model trained with 1920 runs. The black line corresponds to the LAMP prediction for the validation run, the red dashed line denotes the neural network prediction, and the shaded red region represents the uncertainty (2σ) of the neural network from the Monte Carlo dropout method. The validation run identification number for each DoF is also specified to identify if the selected smallest and largest error cases are uniform across the different DoF.

Figure 6 demonstrates that for the validation runs with the smallest L_∞ error, the time-history comparisons between LAMP and the LSTM neural network match well, as is expected from the validation run with the smallest L_∞ error. The neural network predictions in Figure 7 for the validation runs with the largest L_∞ error displays clear deviations between the neural network and LAMP predictions. Figure 7 denotes the runs where the model performed the worst but for each DoF, the predictions match well for the first few wave encounters. Each poorly predicted validation run has a clear phase shift that indicates a large difference between the actual and estimated encounter frame in the neural network methodology. The yaw DoF demonstrates large uncertainty estimates as well, indicating that the model is struggling to predict the ship response with confidence when the ship is deviating too much from the estimated encounter frame.

The work of Silva and Maki (2022) demonstrated that better predictions of the estimated encounter frame help solve this phase shift issue. Future work should attempt to incorporate a wave-specific estimate of the encounter frame with a fast-running low-fidelity simulation tool to at least provide a physics-based estimate due to each individualized wave excitation.

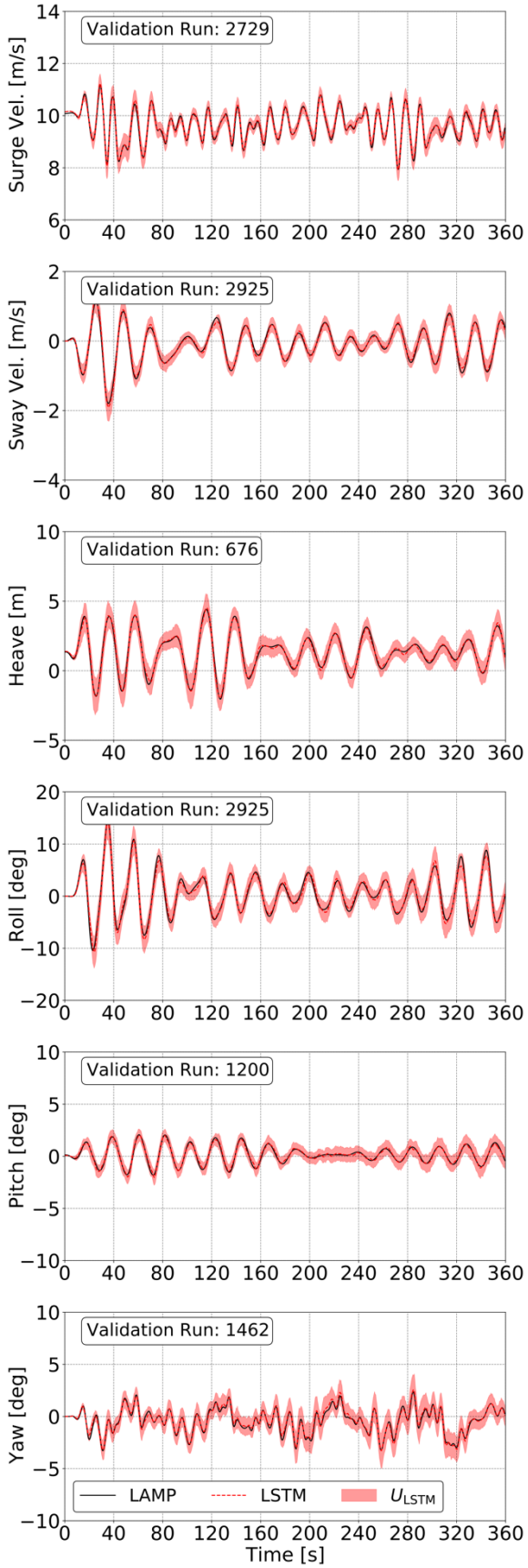

Figure 6. Smallest L_∞ error for the general model trained with 1920 runs.

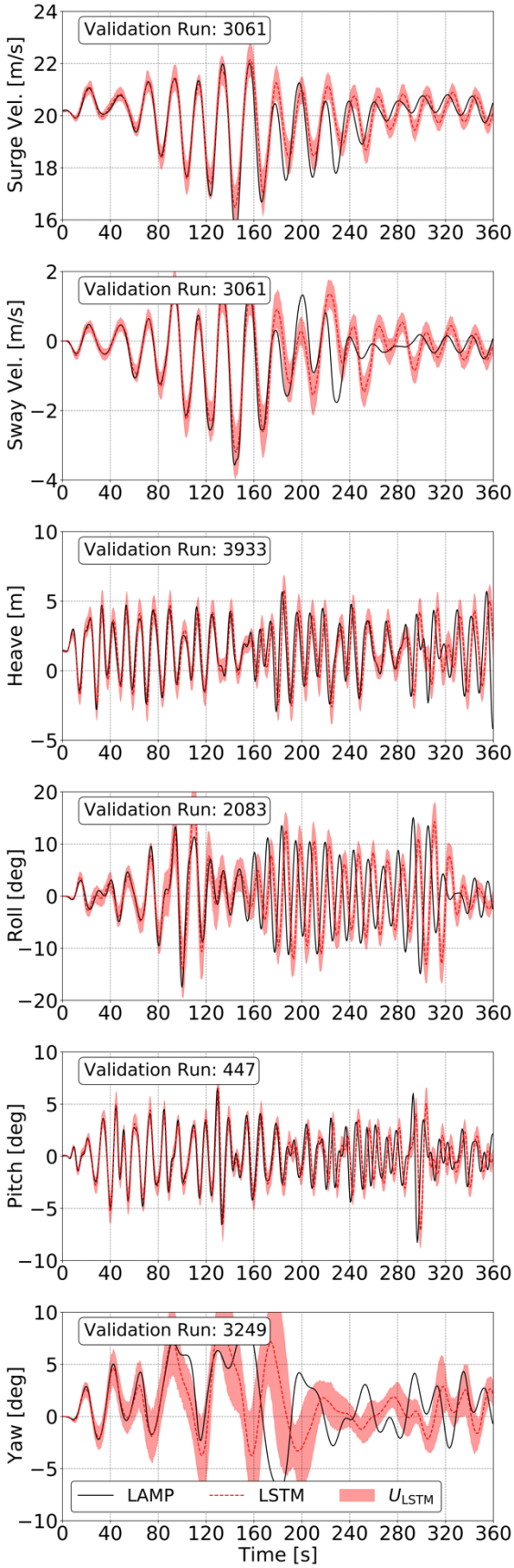

Figure 7. Largest L_∞ error for the general model trained with 1920 runs.

Figure 4 through Figure 7 focused on the evaluation of the neural network model for the 6-DoF response time-histories. Overall, the neural network methodology results in a computationally efficient surrogate model that can predicting the 6-DoF temporal response of a vessel for different speeds and headings. However, the purpose of the CWG method and the broader CWG-CFD-LSTM framework is to identify the critical wave groups for each encounter condition and wave group with shapes described by T_c and j. Therefore, identification of the absolute maximum roll for each run would indicate the effectiveness of the developed surrogate models.

Figure 8 shows LAMP and LSTM general model predictions of the absolute maximum roll for each individual composite wave run for all the speed and heading combinations considered in the current work. The black solid line in Figure 8 denotes a perfect prediction between LAMP and the LSTM model, while each marker corresponds to the LSTM and LAMP prediction of the absolute maximum roll for the same composite wave run.

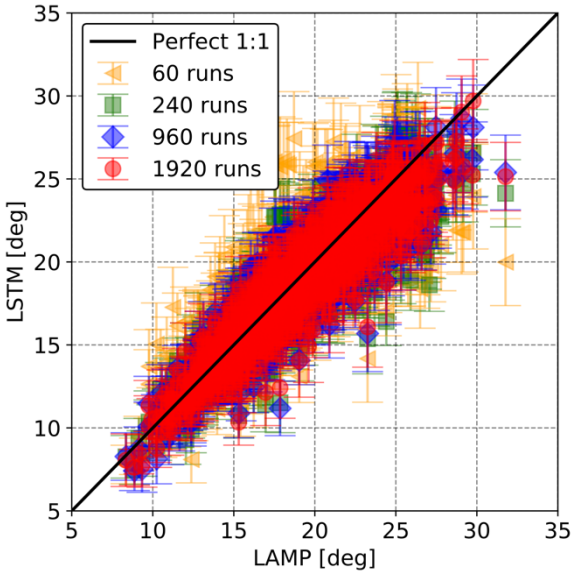

Figure 8. Predictions of absolute maximum roll for each composite wave run for all speeds and headings.

Models with varying quantities of training data were compared in Figure 8 and the error bars correspond to the uncertainty estimate made with the Monte Carlo dropout approach at the moment the absolute maximum occurred. As the quantity of training is increased, the LSTM predictions trend towards the LAMP predictions and the perfect correlation line in Figure 8. Additionally, the size of the error bars decreases indicating a reduction in the uncertainty of the models. Overall, the LSTM models are calculating the absolute maximum roll with accuracy for multiple speeds and headings.

6. CONCLUSION

The CWG-CFD-LSTM framework for free-running vessels was extended to multiple speeds and headings. An ensemble model approach where multiple models were trained, each responsible for one condition, was compared to a general modelling approach where a single model was trained for all speeds and headings. Overall, the general model approach performed better than the ensemble model approach but with sufficient training data both approaches are comparable. The comparability between approaches indicates that the general approach could be extended to even more speeds and headings without the need for large amounts of data at each discrete condition. Therefore, the general approach should be explored in further work developing generalized condition-agnostic frameworks for evaluating extreme events.

Some areas of focus that would improve the presented work are to extend the case study to more operating conditions and seaway descriptions, identify conditions with more severe motions to test the accuracy under even more extreme events, and develop better approximations of the estimated encounter frame that are wave-specific to address the issues when the actual frame deviates significantly from the estimated frame.

7. ACKNOWLEDGMENTS

This work is supported by the Department of Defense (DoD) Science, Mathematics, and Research for Transformation (SMART) scholarship, the Naval Surface Warfare Center Carderock Division (NSWCCD) Extended Term Training (ETT), and the NSWCCD Naval Innovative Science and Engineering (NISE) programs. The authors would also like to acknowledge and thank the Office of Naval Research for the support of this work under contracts N00014-20-1-2096 by the program manager Woei-Min Lin.

8. REFERENCES

Alford, L., 2008, "Estimating Extreme Responses Using a Non-Uniform Phase Distribution", Ph.D. Thesis, The University of Michigan, Ann Arbor, MI.

Anastopoulos, P.A., Spyrou, K.J., 2016, "Ship dynamic stability assessment based on realistic wave group excitations", Ocean Engineering Vol. 120, pp. 256–263.

Anastopoulos, P.A., Spyrou, K.J., Bassler, C.C., Belenky, V., 2016, "Towards an improved critical wave groups method for the probabilistic assessment of large ship motions in irregular seas", Probabilistic Engineering Mechanics Vol. 44, pp. 18–27.

Anastopoulos, P.A., Spyrou, K.J., 2017. "Evaluation of the critical wave groups method for calculating the probability of extreme ship responses in beam seas", In: Proceedings of the 16th International Ship Stability Workshop, Belgrade, Serbia. pp. 131–138.

Anastopoulos, P.A., Spyrou, K.J., 2019, "Evaluation of the critical wave groups method in calculating the probability of ship capsize in beam seas", Ocean Engineering Vol. 187, pp. 106213.

Belenky, V., 1993, "A capsizing probability computation method", Journal of Ship Research Vol. 37, pp. 200–207.

Belenky, V., Campbell, B., 2011, "Evaluation of the Exceedance Rate of a Stationary Stochastic Process by Statistical Extrapolation Using the Envelope Peaks Over Threshold (EPOT) method", Technical Report NSWCCD-50-TR-2011/032, Naval Surface Warfare Center Carderock Division, Hydromechanics Dept, West Bethesda, MD.

Belenky, V., Weems, K.M., Lin, W., Spyrou, K.J., 2010, "Numerical evaluation of capsizing probability in quartering seas with split time method", Proceedings of the 28th Symposium on Naval Hydrodynamics.

Campbell, B., Belenky, V., 2010a, "Statistical extrapolation for evaluation of probability of large roll", Proceedings of the 11th International Symposium on Practical Design of Ships and other Floating Structures.

Campbell, B., Belenky, V., 2010b, "Assessment of short-term risk with Monte-Carlo method", Proceedings of the 11th International Ship Stability Workshop.

Hasselmann, K., Barnett, T., Bouws, E., Carlson, H., Cartwright, D., Enke, K., Ewing, J., Gienapp, H., Hasselmann, D., Kruseman, P., Meerburg, A., Mu¨ller, P., Olbers, D., Richter, K., Sell, W., Walden, H., 1973 "Measurements of wind-wave growth and swell decay during the Joint North Sea Wave Project (JONSWAP)," Deutshes Hydrographisches Institut, Hamburg, Germany.

ITTC, 2011, "Fresh water and seawater properties", ITTC Procedure 7.5-02-01-03, Revision 02, 26th International Towing Tank Conference.

Kingma, D.P., Ba, J., 2014, "Adam: A method for stochastic optimization", arXiv preprint.

Lee, T., Ahn, K., Lee, H., Yum, D., 2003, "On an empirical prediction of hydrodynamic coefficients for modern ship hulls" Proceedings of the International Conference on Marine Simulation and Ship Maneuverability (MARSIM 03).

Lin, W., Meinhold, M., Salvesen, N., Yue, D., 1994, "Large-amplitude motions and waves loads for ship design", Proceedings of the 20th Symposium on Naval Hydrodynamics.

Lin, W.M., Bergquist, J.R., Collette, M.D., Liut, D., Treakle, T.W., Weems, K.M., 2007, "User's guide to the lamp system" Technical report, SAIC, Annapolis, MD.

Mohamad, M.A., Sapsis, T.P., 2018, "Sequential sampling strategy for extreme event statistics in nonlinear dynamical systems", Proceedings of the National Academy of Sciences Vol. 115, pp. 11138-11143.

NATO, 1983, "Standardized Wave and Wind Environments and Shipboard Reporting of Sea Conditions", Standardization Agreement STANAG 4194, North Atlantic Treaty Organization.

Sadat-Hosseini, H., Kim, D., Toxopeus, S., Diez, M., Stern. F., 2015. "CFD and potential flow simulations of fully appended free running 5415m in irregular waves" World Maritime Technology Conference.

Silva, K.M., Maki, K.J., 2021a, "Towards a Computational Fluid Dynamics implementation of the critical wave groups method", Ocean Engineering, Vol. 235, pp. 109451.

Silva, K.M., Maki, K.J., 2021b, "Data-Driven Identification of Critical Wave Groups", Proceedings of the 9th Conference on Computational Methods in Marine Engineering (MARINE 2021), Virtual.

Silva, K.M., Maki, K.J., 2021c, "Critical Wave Group Implementation with Computational Fluid Dynamics and Neural Networks," Proceedings of the 1st International Conference on the Stability and Safety of Ships and Ocean Vehicles (STAB&S 2021), Virtual.

Silva, K.M., Maki, K.J., 2022, "Data-Driven System Identification of 6-DoF Ship Motion in Waves with Neural Networks", Applied Ocean Research (Under Review).

Silva, K.M., Knight, B.G., Maki, K.J., 2022, "Numerical Prediction of Extreme Roll of a Free-Running Ship with Computational Fluid Dynamics and Neural Networks", Proceedings of the International Conference on Decarbonization and Digitalization in Marine Engineering (ICDM 2022), Virtual.

Themelis, N., Spyrou, K.J., 2007, "Probabilistic assessment of ship stability", SNAME Transactions, Vol. 115, pp. 181–206.

Weems, K., Belenky, V., Spyrou, K., Aram, S., Silva, K., 2020, "Towards numerical estimation of probability of capsizing caused by broaching-to", Proceedings of the 33rd Symposium on Naval Hydrodynamics.

Xu, W., Silva, K.M., Maki, K.J., 2021, "A data-driven model for nonlinear marine dynamics," Ocean Engineering, Vol. 236, pp. 109469.